

# Preparation of yttria-stabilized zirconia (YSZ) films on $\text{La}_{0.85}\text{Sr}_{0.15}\text{MnO}_3$ (LSM) and LSM–YSZ substrates using an electrophoretic deposition (EPD) process

Fanglin Chen, Meilin Liu \*

*School of Materials Science and Engineering, Georgia Institute of Technology, Atlanta, GA 30332, USA*

Received 27 April 2000; received in revised form 29 June 2000; accepted 8 July 2000

---

## Abstract

Preparation of high-quality yttria-stabilized zirconia (YSZ) electrolyte films on porous substrates is critical to the fabrication of high-performance solid-state ionic devices such as fuel cells and gas sensors. An electrophoretic deposition (EPD) process is investigated for the preparation of YSZ electrolyte films on both porous  $\text{La}_{0.85}\text{Sr}_{0.15}\text{MnO}_3$  (LSM) and porous LSM–YSZ composite substrates. The Pechini process is used for the preparation of fine LSM powders with an average particle size of about 0.1  $\mu\text{m}$ . The processing parameters critically influencing the microstructures of green YSZ films are identified and optimized to obtain uniform, crack-free green YSZ films with high packing density of fine YSZ particles. Dense YSZ films with a thickness of about 10  $\mu\text{m}$  have been successfully fabricated on both porous LSM and porous LSM–YSZ substrates when sintered at 1250°C for 2 h. © 2001 Elsevier Science Ltd. All rights reserved.

*Keywords:* Electrophoretic deposition; Films; Fuel cells; (La,Sr)MnO<sub>3</sub>; ZrO<sub>2</sub>

---

## 1. Introduction

Solid oxide fuel cells (SOFCs) have emerged as a leading technology to provide clean and efficient power sources of the future. The advantages offered by the operation of SOFCs at low or intermediate (600–800°C) temperatures, such as high energy efficiency and reduced material and maintenance cost, have stimulated intense investigations into new materials with fast transport and high catalytic activities and new processes for fabrication of thin film SOFCs.<sup>1,2</sup>

Yttria-stabilized zirconia (YSZ) is still the best electrolyte among all solid electrolytes studied for SOFCs because of its excellent long-term stability, mechanical strength and durability. Due to its limited ionic conductivity, however, YSZ must be fabricated in a thin-film form for intermediate or low temperature SOFCs. A number of techniques have been successfully developed for preparation of YSZ films on porous substrates, including electrochemical vapor deposition (EVD),<sup>3</sup>

chemical vapor deposition (CVD),<sup>4</sup> physical vapor deposition (PVD),<sup>5</sup> electrostatic spray deposition,<sup>6</sup> sputter deposition,<sup>7</sup> sol–gel processing,<sup>8</sup> solution deposition<sup>9</sup> and colloidal deposition.<sup>10</sup> However, each of these processes has some limitations, including difficulty in obtaining good compositional homogeneity, not suitable for mass production, not cost-effective, or difficult to reproduce.

Another alternative thin-film forming approach is electrophoretic deposition (EPD),<sup>11</sup> in which charged particles dispersed in a stable suspension are driven by a dc electric field to move towards an oppositely charged electrode, upon which they ultimately deposit and build up a closely-packed particulate layer. EPD is a combination of two processes: electrophoresis and deposition. Electrophoresis is the motion of charged particles in a suspension under the influence of an electric field. Deposition is the coagulation of charged particles to a dense mass. As the green ware contains no organics, no burn out procedures are required. EPD is inexpensive and has been used for many years to fabricate green ceramic bodies and coatings with different shapes for applications ranging from ceramic/ceramic and metal/ceramic composites to thin/thick film coatings for

---

\* Corresponding author. Tel.: +1-404-894-6114; fax: +1-404-894-9140.

*E-mail address:* [meilin.liu@mse.gatech.edu](mailto:meilin.liu@mse.gatech.edu) (M. Liu).

electronic devices.<sup>12,13</sup> EPD has the advantages of short formation times, little restriction in the shape of substrates, simple deposition apparatus, and suitable for mass production. It is a cost-effective, reproducible process for the preparation of electrolyte films for SOFCs. However, gas tight films are difficult to obtain by EPD from aqueous suspensions due to the evolution of hydrogen and oxygen by water electrolysis at the substrate, resulting in the formation of holes in the film. Fortunately, this can be avoided by using organic solvents such as ketones or ethanol to form the suspension.

The preparation of YSZ films for ceramic coatings using EPD was first investigated by Nicholson and co-workers.<sup>14,15</sup> YSZ films as thin as 2  $\mu\text{m}$  were deposited on a graphite cathode from YSZ-ethanol suspensions using constant current EPD. Ishihara and co-workers<sup>16</sup> applied EPD to deposit YSZ films onto a porous NiO–CaO-stabilized zirconia (NiO–CSZ) cermet using ketone as the solvent. Since the conductivity of the NiO–CSZ cermet was very low, a Pt electrode was plated on one face of the cermet using electroless-plating prior to the deposition of YSZ powder. The deposition was conducted at a constant voltage of 5 V for 3 min and the process was repeated five times to yield a 5  $\mu\text{m}$  non-porous YSZ film after being sintered at 1375°C for 1 h.

In this article, we report our findings in fabricating YSZ films on porous  $\text{La}_{0.85}\text{Sr}_{0.15}\text{MnO}_3$  (LSM) substrates using an EPD process. LSM is superior to NiO–CSZ cermet as the substrate because LSM is conductive. Further, LSM–YSZ composite was also used as substrate for deposition of YSZ films because the addition of YSZ to the LSM electrode significantly enhances the catalytic activity of the LSM–YSZ composite electrode.<sup>17</sup> Another anticipated benefit of using the composite substrate is the improved adhesion between the film and the substrate due to the intimate sintering of YSZ particles to the LSM–YSZ substrate. The processing parameters affecting the film microstructure are systematically investigated and subsequently optimized to improve the quality of films. The electrochemical properties of the films and the performance of the solid-state ionic devices based on these films will be discussed in future communications.

## 2. Experimental

### 2.1. Preparation of LSM and LSM–YSZ substrates

LSM powders were prepared using the Pechini process, as summarized in Fig. 1. The precursors were  $\text{La}(\text{NO}_3)_3 \cdot 4\text{H}_2\text{O}$  (Alfa),  $\text{Mn}(\text{CH}_3\text{COO})_2 \cdot 4\text{H}_2\text{O}$  (Aldrich), and  $\text{Sr}(\text{NO}_3)_2$  (Aldrich). Stoichiometric amount of the nitrates (yielding the composition of  $\text{La}_{0.85}\text{Sr}_{0.15}\text{MnO}_3$ ) was dissolved into de-ionized water. 90/10 mole ratio of citric acid/ethylene glycol was first dissolved in

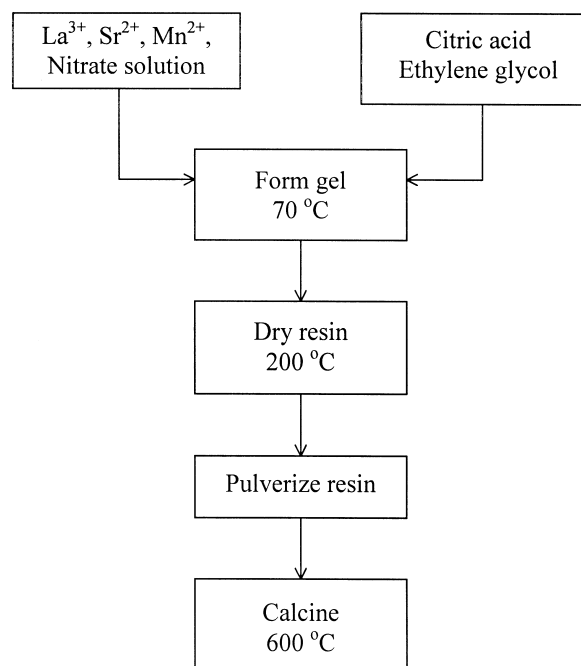


Fig. 1. A flow chart of the Pechini process for preparation of LSM powders.

de-ionized water and then mixed with the nitrate solution. The solution was heated to 70°C under continuous stirring until it turned into a gel. The gel was dried at 200°C and the resulting resin was pulverized and calcined at 600°C for 1 h. The calcined powder was characterized using powder X-ray diffraction (XRD, Scintag X1). The specific surface area of the LSM powders was determined using a BET surface area analyzer (Coulter SA 3100). The morphology and particle size of the LSM powders were characterized using a transmission electron microscope (TEM, Hitachi HF 2000). The particle size distribution was determined using a laser scattering technique (Coulter DELSA 440SX).

LSM–YSZ composite powders were mixed through ball-milling of 80/20 (weight ratio) LSM and YSZ (TOSOH TZ-8Y) powders in ethanol for 24 h using  $\text{ZrO}_2$  balls as milling media. The LSM and LSM–YSZ powders were then pressed into pellets (diameter 20 mm, pressure 200 MPa) with 5 wt.% PVA as binder and subsequently fired at 700°C for 0.5 h to remove the binder. The surfaces of the fired pellets were grounded using SiC 4000 paper prior to an EPD process.

### 2.2. EPD of YSZ on LSM and LSM–YSZ composite substrates

YSZ suspension was obtained by dispersing YSZ powders with iodine in acetylacetone, acetone, ethanol, or a mixture of acetone and ethanol (volume ratio of 3/1). The zeta potentials and conductivities of the YSZ suspensions in different solvents were measured using an

electrophoretic light scattering technique (Coulter DELSA 440SX). The pH value of the YSZ suspension was monitored using a pH meter (Cole Parmer Model 59002-00). In a typical deposition, 1.8 g YSZ and 0.9 g  $I_2$  were added to a 250 ml beaker with 150 ml acetone and 50 ml ethanol. The mixture was ultrasonicated with a high intensity ultrasonic probe (GE 130 Ultrasonic processor) to form a stable suspension. The experimental arrangement for EPD is schematically illustrated in Fig. 2. LSM or LSM–YSZ substrate was loaded on one side of the Teflon deposition cell acting as the cathode while a Pt disk was mounted on the opposite side of the cell acting as the anode. The surface areas of the deposition substrate and the Pt disk are 3.6 and 4.5  $cm^2$ , respectively. The two electrodes were kept parallel at 1.5 cm apart in the Teflon deposition cell, which was placed in the YSZ suspension under gentle continuous stirring to ensure the uniformity of the suspension and to minimize the sedimentation of YSZ particles during deposition. Positively charged YSZ particles were then electrophoretically deposited onto the cathode, at a constant deposition voltage varied in the range from 5 to 40 V with a deposition time from 3 to 30 min. Green YSZ film obtained in each case was dried in air overnight and the surface morphology was characterized using a scanning electron microscope (SEM Hitachi S-800). Crack-free green YSZ films deposited on LSM and LSM–YSZ substrates were sintered to temperatures from 1200 to 1300°C for 2 h, with a heating rate of 2, 5, 10 and 15°C/min, respectively. The surface and cross section of the sintered YSZ films were characterized using an SEM.

### 3. Results and discussion

#### 3.1. Characteristics of the LSM powder obtained from the Pechini process

Shown in Fig. 3(a) is a XRD pattern obtained for the LSM powder after calcination at 600°C for 1 h, indicating that the powder has a pure perovskite phase. The average particle size is about 100 nm, as calculated from the line broadening according to Scherrer formula.<sup>18</sup> Shown in Fig. 3(b) is a representative TEM image of the LSM powder, showing that the average particle size is about 100 nm. The BET surface area of the LSM powder is 37  $m^2/g$ , as determined from the surface area analyzer. Shown in Fig. 3(c) is the particle size distribution of the LSM powder, with an average particle size of 105 nm, as obtained from the laser scattering technique. The narrow particle size distribution of LSM powder may enhance uniform distribution of electrical field near substrate surface during EPD.

#### 3.2. Effect of the solvents on YSZ suspensions

For a constant-voltage deposition, the weight ( $w$ ) of charged particles deposited per unit area of the electrode in the initial period can be expressed as:<sup>16</sup>

$$w = \frac{2}{3} C \varepsilon_0 \varepsilon_r \xi \eta^{-1} E L^{-1} t \quad (1)$$

where  $C$  represents the concentration of the particle in the suspension,  $\varepsilon_0$  the permittivity of vacuum,  $\varepsilon_r$  the

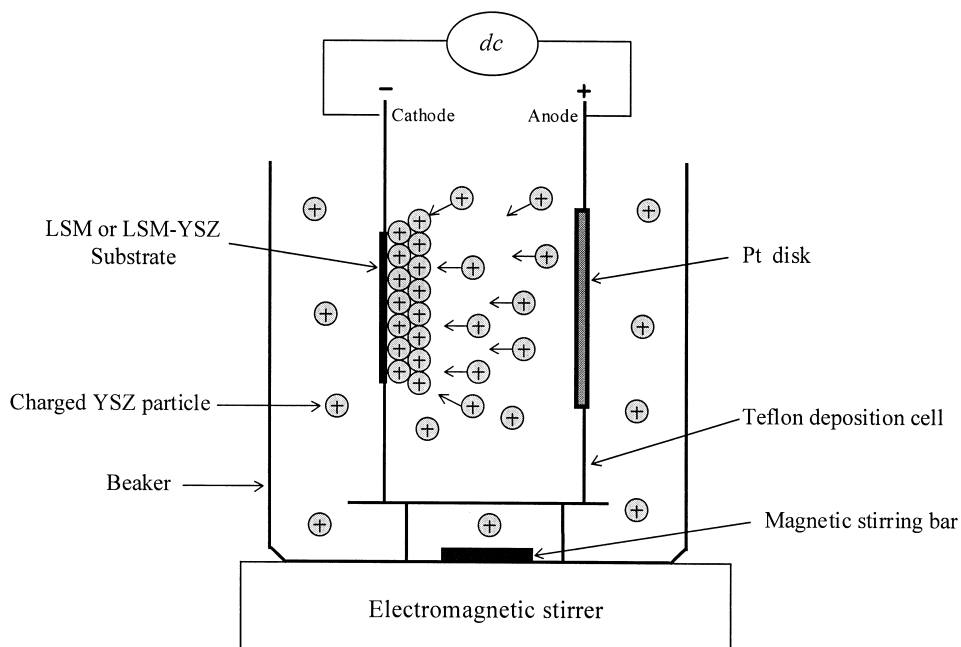


Fig. 2. A schematic diagram showing the cell configuration for EPD of YSZ on LSM or LSM–YSZ substrates.

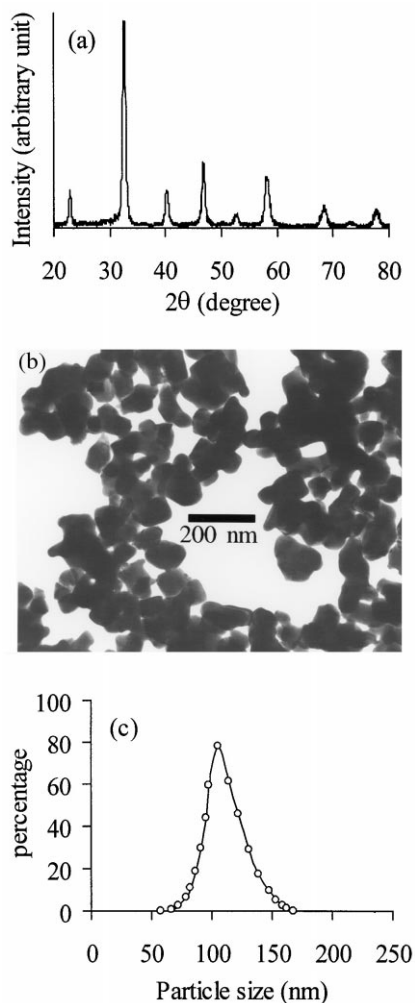


Fig. 3. Characteristics of the LSM powder derived from the Pechini process after being calcined at 600°C for 1 h: (a) a XRD pattern, (b) a TEM micrograph, and (c) the particle size distribution.

relative permittivity of the solvent,  $\xi$  the zeta potential of the particle,  $\eta$  the viscosity of the solvent,  $E$  the applied potential,  $L$  the distance between electrodes, and  $t$  the deposition time. If the solvent, the particles, and the apparatus for EPD are fixed,  $\epsilon_r$ ,  $\eta$ ,  $\xi$  and  $L$  are constants and the weight of deposited particles ( $w$ ) is determined by  $C$ ,  $E$  and  $t$ . Thus, the mass of deposited particles and the thickness of the deposited films can be readily controlled by the concentration of the suspension ( $C$ ), applied potential ( $E$ ), and the deposition time ( $t$ ). Due to the high resistivity of the YSZ deposit, however, the voltage drop per unit length decreases with deposition time and the velocity of the charged particles gradually decreases. Accordingly, it is anticipated that the deposited mass will initially increase linearly with the deposition time, but will gradually deviate from the linear dependence later on.

The zeta potential of the YSZ suspension as a function of the concentration of  $I_2$  added in different solvents is shown in Fig. 4. It can be seen that the zeta

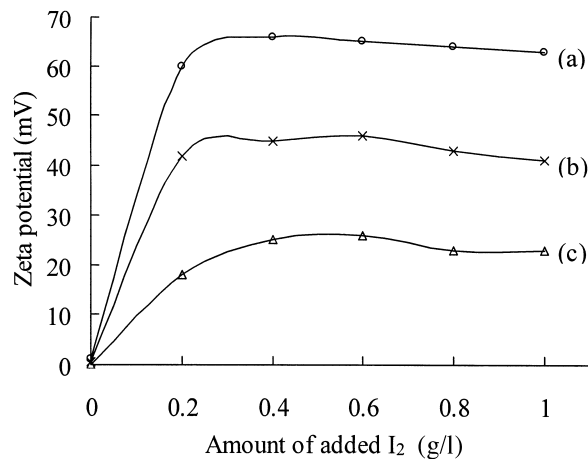


Fig. 4. Zeta potential of the YSZ suspension as a function of the concentration of  $I_2$  added in (a) acetone, (b) acetylacetone, and (c) ethanol. The YSZ concentration in the suspensions was 9.0 g/l.

potentials of the YSZ suspensions in acetone and acetylacetone are relatively high, indicating that these suspensions are suitable for EPD to form YSZ film, since a large zeta potential will result in a fast deposition rate, as predicted from Eq. (1). The zeta potential of the YSZ suspension in ethanol is relatively low, implying a much slower deposition rate using this suspension. It can also be seen that the zeta potentials are almost independent of the  $I_2$  concentration when the  $I_2$  concentration is greater than 0.4 g/l in the suspensions.

The quality of the green YSZ films prepared using EPD was found to depend strongly on the solvents used. The green YSZ films obtained were of non-uniform with many cracks when acetylacetone was used as the solvent. Further, the substrate was attacked by the solvent, leading to film delamination. When acetone was used as the solvent, the deposited YSZ film was uniform with a smooth surface when it was taken out of the suspension. However, the film cracked into small pieces during drying at room temperature, due possibly to the poor adhesion of the YSZ film to the substrate and to the high evaporating rate of acetone. Although the deposited YSZ film was quickly transferred into a container with saturated acetone atmosphere, cracks can not be completely eliminated in the dry green YSZ films. When ethanol was used as the solvent, the deposition rate was very slow compared with that in acetone. The film was thin and non-uniform since the YSZ powders falling down from the top to the bottom of the film when it was taken out from the suspension. However, the film was still continuous and there were no cracks, probably because ethanol has a much slower evaporating rate than acetone. To compromise, a mixture of acetone and ethanol (volume ratio of 3/1) was used as the solvent in our EPD experiment and good quality YSZ films with high packing density of YSZ fine particles were obtained.

### 3.3. Effect of $I_2$ concentration in the suspension

Shown in Fig. 5 are the zeta potential, conductivity, and the pH value of the suspension as well as the deposited YSZ mass as a function of the concentration of  $I_2$  in the suspension using a mixture of acetone and ethanol as the solvent. Although the zeta potential of YSZ particles was almost 0 in the acetone/ethanol mixture, it increased rapidly with the addition of  $I_2$  and attained a constant potential of 60 mV when the  $I_2$  concentration was greater than 0.4 g/l. The pH value of the suspension decreased with the increase of  $I_2$  concentration in the suspension. This suggests that free protons be formed according to the following reactions between  $I_2$  and the solvent.<sup>19</sup>

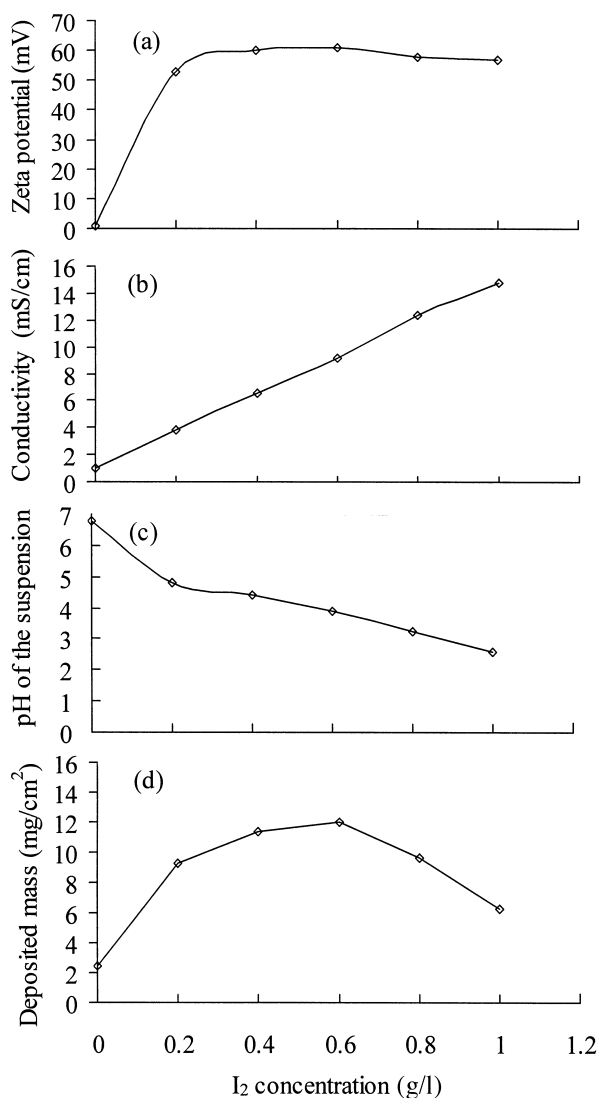
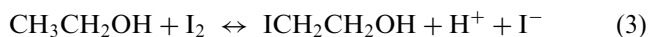
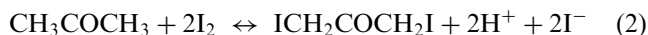


Fig. 5. The effect of  $I_2$  concentration in the suspension on (a) zeta potential, (b) conductivity, (c) pH value, and (d) YSZ mass deposited at 20 V for 8 min. The solvent was a mixture of acetone/ethanol (volume ratio 3/1) and YSZ concentration was 9.0 g/l.

The protons generated were adsorbed on the suspended YSZ particles, making them positively charged. Application of a dc field forced the positively charged YSZ particles to move towards and deposited on the cathode. The amount of protons increased with the increase of the  $I_2$  concentration in the suspension, resulting in an increase of the zeta potential of YSZ particles and a decrease of the pH value in the suspension. Since the amount of deposited YSZ particles increases with the increase in zeta potential of the YSZ particles in the suspension, as implied by Eq. (1), the amount of YSZ deposited would initially increase with increasing  $I_2$  concentration and subsequently attain a constant. However, Fig. 5(d) shows that the deposited YSZ weight increased with  $I_2$  concentration, attained a maximum at  $I_2$  concentration of 0.6 g/l and then decreased with the increase of the  $I_2$  concentration in the suspension. This is because the charge carried by the free ions in the suspension was ignored in deriving Eq. (1). The zeta potential of the suspension was almost independent of the  $I_2$  concentration above 0.4 g/l, as shown in Fig. 5(a). The electrical conductivity of the YSZ suspension increased linearly with increasing the amount of added  $I_2$ , as shown in Fig. 5(b). Therefore, it may be concluded that the amount of free protons increased with the increase of  $I_2$  concentration. This is further confirmed by the continuous decrease in the pH value of the YSZ suspension with the increase of  $I_2$  concentration, as shown in Fig. 5(c). As a result, the formed free protons carried some electrical charges, since the mobility of free protons is far higher than that of charged YSZ particles. Consequently, an excess amount of  $I_2$  enhanced proton conduction and decreased the amount of YSZ deposited. Therefore, the YSZ suspension with an  $I_2$  concentration of 0.6 g/l seems to be desirable because of the highest deposition rate. Under this condition, the amount of free protons was negligibly small and the YSZ particles seem to be the major charge carriers in the suspension. Accordingly, the amount of  $I_2$  added to the suspension was kept at 0.6 g/l in our subsequent studies.

### 3.4. Effect of the substrates

The uniformity and conductivity of the substrate is critical to the quality of the deposited green YSZ film. When the as-pressed LSM or LSM–YSZ composite pellets were used as substrates for EPD, the deposition rate was slow and the obtained film was non-uniform. This is due primarily to the high resistance of the substrates resulting from the binder added. When the

pellets were fired at 700°C for 0.5 h, the binder was burnt off and the conductivity of the substrates increased substantially. Consequently green YSZ films of high quality were obtained on the fired and surface-grounded LSM and LSM–YSZ substrates. Under the same conditions, the deposition rate on an LSM–YSZ composite substrate is a little bit slower than that on an LSM substrate, due primarily to the slightly higher resistance of the LSM–YSZ composite substrate.

### 3.5. Effect of deposition conditions on deposition rate

Fig. 6(a) shows the mass of YSZ film deposited on LSM substrate at 20 V for 8 min as a function of the YSZ particle concentration in the suspension with  $I_2$  concentration kept at 0.6 g/l. The weight of the deposited

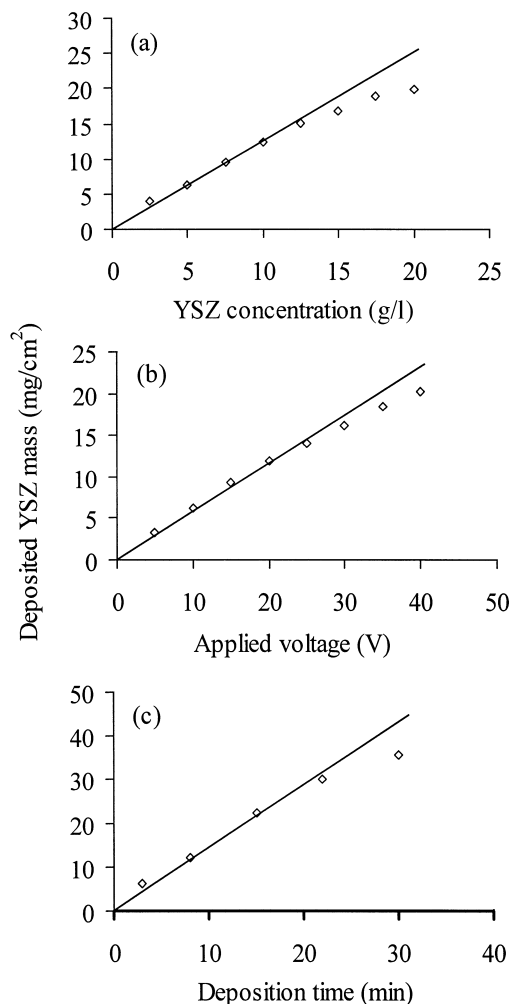


Fig. 6. Effect of deposition conditions on deposition rate: (a) dependence on the YSZ concentration in the suspension, with applied voltage 20 V, deposition time 8 min, and  $I_2$  concentration 0.6 g/l; (b) dependence on the applied voltage, with deposition time 8 min, YSZ concentration 9.0 g/l, and  $I_2$  concentration 0.6 g/l; and (c) dependence on deposition time, with applied voltage 20 V, YSZ concentration 9.0 g/l, and  $I_2$  concentration 0.6 g/l.

YSZ film increased linearly with the increase of the YSZ concentration in the suspension when the YSZ concentration was below 15 g/l, but there was some slight deviation at higher YSZ concentration. It was also found that the YSZ concentration higher than 10 g/l resulted in poor quality non-uniform green YSZ films. This is due probably to the high deposition rate and the agglomeration of YSZ particles at high YSZ concentration, leading to poor packing density of the green YSZ film. However, if the YSZ concentration in the suspension was smaller than 5 g/l, the deposition rate was very slow. Therefore, the concentration of YSZ particles was kept at 9.0 g/l in subsequent studies to ensure both fast deposition rate and uniform and smooth green YSZ films.

According to Eq. (1), the deposition rate or the thickness of the deposited YSZ film would increase linearly with the applied voltage, if all other parameters were held constant. Fig. 6(b) illustrates the amount of YSZ deposited for 8 min under different applied voltages. A linear relationship between the deposited YSZ mass and the applied voltage was obtained when the applied voltage was lower than 30 V. However, deviation from the linear behavior was observed at applied voltages higher than 30 V. High applied voltage also led to inhomogeneity of the green YSZ film. Consequently, a voltage of 20 V was adopted in the subsequent study.

The weight of the deposited YSZ film increased linearly with the deposition time within the first 15 min, but deviation from the linearity occurred at prolonged deposition period, as shown in Fig. 6(c). In a constant-voltage EPD, while the potential between the electrodes

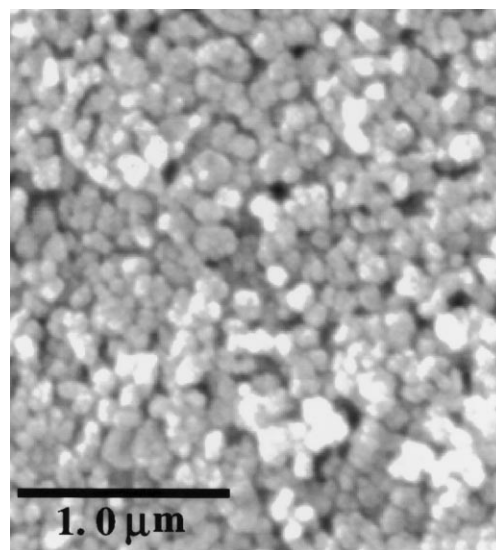


Fig. 7. A typical surface view of a green YSZ film deposited on an LSM substrate using an EPD process under optimal conditions: YSZ concentration of 9.0 g/l dispersed in a mixture of acetone/ethanol (volume ratio 3/1),  $I_2$  concentration of 0.6 g/l, a dc voltage of 20 V, and a deposition time of 8 min.

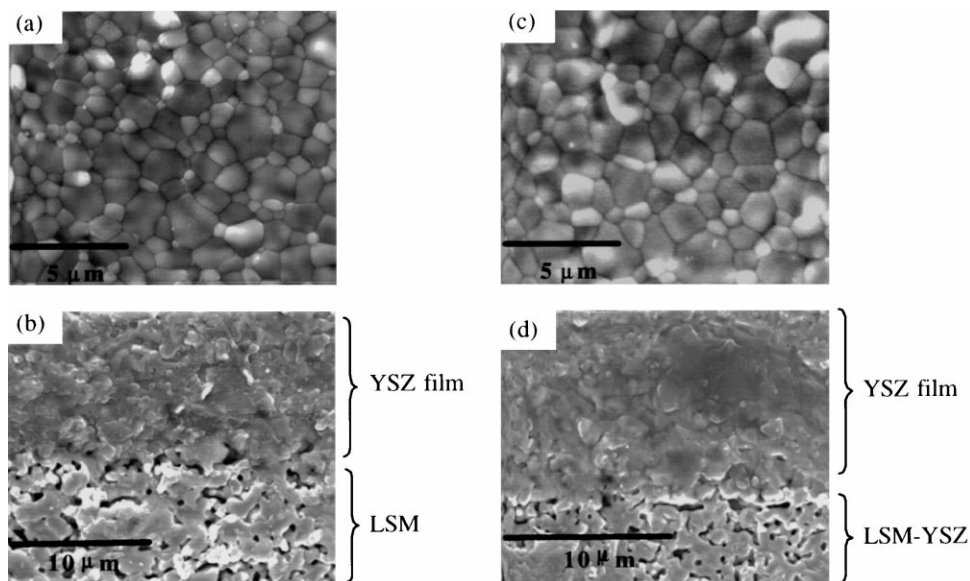


Fig. 8. Surface (a and c) and cross-sectional (b and d) microstructures of the YSZ films sintered at 1250°C for 2 h with a heating rate of 10°C/min: (a) and (b) on LSM substrate whereas (c) and (d) on LSM–YSZ substrate.

is maintained constant, the electric field influencing electrophoresis decreases with deposition time because of the formation of an insulating YSZ film. The deposition rate may approach zero if the potential gradient is too flat, because deposition requires a steeper potential gradient than electrophoresis. Therefore, it is expected that the deposited YSZ layer as well as the agglomerated ions, protons, would suppress the subsequent electrophoretic deposition as the deposition period is prolonged. However, the initially linear relationship between the deposited YSZ mass and the deposition time, as shown in Fig. 6(c), indicates that these effects are negligible within the first 15 min. However, it was found that when the deposition time was longer than 10 min, thick green YSZ film of poor quality (non-uniform) was obtained. A deposition time of 8 min seemed to be optimal, yielding a smooth green YSZ film with uniform thickness and high packing density.

### 3.6. Microstructure characterization of the YSZ films

Shown in Fig. 7 is a representative surface view of a green YSZ film deposited on an LSM substrate using EPD under optimal conditions: a YSZ concentration of 9.0 g/l dispersed in a mixture of acetone and ethanol (volume ratio of 3/1), an  $I_2$  concentration of 0.6 g/l, a dc voltage of 20 V, and a deposition time of 8 min. It can be seen that the surface of the green YSZ film is smooth, crack-free, and uniform. The average size of the YSZ particles is 0.1  $\mu\text{m}$ . The fine YSZ particles are uniformly distributed.

The sintering temperature and the heating rate are critical to obtain dense, pinhole and crack free YSZ films. The heating rates were 2, 5, 10 and 15°C/min and

the sintering temperatures were varied from 1200 to 1300°C. It was found that a slow heating rate (2 or 5°C/min) resulted in only porous YSZ films even when sintered at 1300°C. Dense YSZ films could be achieved by sintering at 1250 and 1300°C of the green YSZ film on both LSM and LSM–YSZ substrates with a high heating rate (10 or 15°C/min). The high heating rate might suppress YSZ particle growth below the sintering temperature.

Shown in Fig. 8 are the typical surface and cross-sectional views of the YSZ films on LSM and LSM–YSZ substrates sintered at 1250°C for 2 h with a heating rate of 10°C/min. It can be seen that the YSZ films on both substrates are dense, crack and pinhole-free with an average thickness of 10  $\mu\text{m}$ . Such a low temperature to achieve dense YSZ film may be the result of the high quality green YSZ film obtained from EPD. Both LSM and LSM–YSZ substrates are porous with a porosity of about 20%, making them suitable as cathodes in SOFCs.

## 4. Conclusions

The Pechini process has been used to prepare fine LSM powders with an average particle size of about 0.1  $\mu\text{m}$ . Both porous LSM and porous LSM–YSZ pellets are used as substrates for preparation of YSZ films using an EPD process. Uniform, crack-free green YSZ films with high packing density of YSZ particles are obtained by optimizing the key processing variables. Dense, crack and pinhole-free sintered YSZ films with a thickness of about 10  $\mu\text{m}$  have successfully been prepared using an one-step EPD on both porous LSM and

porous LSM–YSZ substrates at a sintering temperature of 1250°C.

### Acknowledgements

The authors wish to gratefully acknowledge partial support of this project by the National Science Foundation under Award No. DMR-9357520, by Georgia Tech Research Cooperation, and by the Georgia Institute of Technology Molecular Design Institute, under prime contract N00014-95-1-1116 from the Office of Naval Research. Special thanks are given to Dr Z. L. Wang at Georgia Institute of Technology Electron Microscope Center for SEM assistance.

### References

1. Minh, N. Q. and Takahashi, T., *Science and Technology of Ceramic Fuel Cells*. Elsevier, New York, 1995, pp. 1–2.
2. Badwal, S. P. S. and Foger, K., Solid oxide electrolyte fuel cell review. *Ceramics International*, 1996, **22**, 257–265.
3. (a) Pal, U. B. and Singhal, S. C., Electrochemical vapor deposition of yttria-stabilized zirconia film. *J. Electrochem. Soc.*, 1990, **137**, 2937–2941; (b) Suzuki, M., Sasaki, H., Otoshi, S., Kajimura, A., Sugiura, N. and Ippommatsu, M., High performance solid oxide fuel cell cathode fabricated by electrochemical vapor deposition. *J. Electrochem. Soc.*, 1994, **141**, 1928–1931; (c) Singhal, S. C., Recent progress in tubular solid oxide fuel cell technology. In *Proceedings of the Fifth International Symposium on Solid Oxide Fuel Cells (SOFC-V)*, ed. U. Stimming, S. C. Singhal, H. Tagawa and W. Lehnert. The Electrochemical Society, Pennington, NJ, 1997, pp. 37–50.
4. Cao, G. Z., Brinkman, H. W., Meijerink, J., De Vries, K. J. and Burggraaf, A. J., Pore narrowing and formation of ultrathin yttria-stabilized zirconia layers in ceramic membranes by chemical vapor/electrochemical vapor deposition. *J. Am. Ceram. Soc.*, 1993, **76**, 2201–2208.
5. Unal, O., Mitchell, T. E. and Heuer, A. H., Microstructures of Y<sub>2</sub>O<sub>3</sub>-stabilized ZrO<sub>2</sub> electron beam-physical vapor deposition coating on Ni-base superalloys. *J. Am. Ceram. Soc.*, 1994, **77**, 984–992.
6. Chen, C. H., Nord-Varhaug, K. and Schoonman, J., Coating of yttria-stabilized zirconia (YSZ) thin films on Gadolinia-doped ceria (GCO) by the electrostatic spray deposition (ESD) technique. *Journal of Materials Synthesis and Processing*, 1996, **4**, 189–194.
7. Tsai, T. and Barnett, S. A., Bias sputter deposition of dense yttria-stabilized zirconia films on porous substrates. *J. Electrochem. Soc.*, 1995, **142**, 3084–3087.
8. Mehta, K., Xu, R. and Virkar, A. V., Two-layer fuel cell electrolyte structure by sol–gel processing. *J. Sol–gel Sci. and Tech.*, 1998, **11**, 203–207.
9. Chen, C. C., Nasrallah, M. M. and Anderson, H. U., Synthesis and characterization of YSZ thin film electrolytes. *Solid State Ionics*, 1994, **70/71**, 101–108.
10. De Souza, S., Visco, S. J. and De Jonghe, L. C., Reduced-temperature solid oxide fuel cell based on YSZ thin-film electrolyte. *J. Electrochem. Soc.*, 1997, **144**, L35–L37.
11. Sarkar, P. and Nicholson, P. S., Electrophoretic deposition (EPD): mechanisms, kinetics, and application to ceramics. *J. Am. Ceram. Soc.*, 1996, **79**, 1987–2002.
12. Tassel, J. V. and Randall, C. A., Electrophoretic deposition and sintering of thin/thick PZT films. *J. Eur. Ceram. Soc.*, 1999, **19**, 955–958.
13. Maiti, H. S., Datta, S. and Basu, R. N., High-Tc superconductor coating on metal substrate by an electrophoretic technique. *J. Am. Ceram. Soc.*, 1989, **72**, 1733–1735.
14. Sarkar, P., Huang, X. and Nicholson, P. S., Zirconia/alumina functionally gradient composites by electrophoretic deposition. *J. Am. Ceram. Soc.*, 1993, **76**, 1055–1056.
15. Sarkar, P., Prakash, O., Wang, G. and Nicholson, P. S., Microlaminate ceramic/ceramic composites (YSZ/Al<sub>2</sub>O<sub>3</sub>). *Ceram. Eng. Sci. Proc.*, 1994, **15**, 1019–1027.
16. Ishihara, T., Sato, K. and Takita, Y., Electrophoretic deposition of Y<sub>2</sub>O<sub>3</sub>-stabilized ZrO<sub>2</sub> electrolyte films in solid oxide fuel cells. *J. Am. Ceram. Soc.*, 1996, **79**, 913–919.
17. Wang, S., Jiang, Y., Zhang, Y., Yan, J. and Li, W., The role of 8 mole% yttria stabilized zirconia in the improvement of electrochemical performance of lanthanum manganite composite electrodes. *J. Electrochem. Soc.*, 1998, **145**, 1932–1939.
18. Cullity, B. D., *Elements of X-ray Diffraction*. Addison-Wesley, Reading, MA, 1978, p.102.
19. Okumura, S., Tsukamoto, T. and Koura, N., Fabrication of ferroelectric BaTiO<sub>3</sub> films by electrophoretic deposition. *Jpn. J. Appl. Phys.*, 1993, **32**, 4182–4185.